

Critical structure and emergent symmetry of Dirac fermion systems

Jiang Zhou^{1,*}

¹*Department of Physics, Guizhou University, Guiyang 550025, PR China*

Emergent symmetry in Dirac system means that the system acquires an enlargement of two basic symmetries at some special critical point. The continuous quantum criticality between the two symmetry broken phases can be described within the framework of Gross-Neveu-Yukawa (GNY) model. Using the first-order ϵ expansion in $4 - \epsilon$ dimensions, we study the critical structure and emergent symmetry of the chiral GNY model with N_f flavors of four-component Dirac fermions coupled strongly to an $O(N)$ scalar field under a small $O(N)$ -symmetry breaking perturbation. After determining the stable fixed point, we calculate the inverse correlation length exponent and the anomalous dimensions (bosonic and fermionic) for general N and N_f . Further, we discuss the emergent-symmetry and the emergent supersymmetric critical point for $N \geq 4$ on the basis of $O(N)$ -GNY model. It turns out that the chiral emergent- $O(N)$ universality class is physically meaningful if and only if $N < 2N_f + 4$. On this premise, the small $O(N)$ -symmetry breaking perturbation is always irrelevant in the chiral emergent- $O(N)$ universality class. Our studies show that the emergent symmetry in Dirac systems has an upper boundary $O(2N_f + 3)$, depending on the flavor numbers N_f . As a result, the emergent- $O(4)$ and $O(5)$ symmetries are possible to be found in the systems with fermion flavor $N_f = 1$, and the emergent- $O(4)$, $O(5)$, $O(6)$ and $O(7)$ symmetries are expected to be found in the systems with fermion flavor $N_f = 2$. Our result also suggests some rich transitions with emergent- $Z_2 \times O(2) \times O(3)$ symmetry and so on. Interestingly, in the emergent- $O(4)$ universality class, there is a supersymmetric critical point which is expected to be found in the systems with fermion flavor $N_f = 1$.

I. INTRODUCTION

In quantum field theory, the Gross-Neveu model is a fundamental model of half spin fermions and contains a quartic self-interaction of fermion fields[1–3]. It has some interesting properties which are commonly shared by the quantum chromodynamics[1]. For example, the phenomena of asymptotic freedom and dynamical symmetry breaking. Due to its close connections with the phase transitions in graphene, the general Gross-Neveu theory is also of interest in condensed matter theory. For instance, it has been suggested that the transition from the semimetal to the Mott-insulating phase in graphene can be described by what is termed chiral Gross-Neveu model[4–11]. Based on the specific interaction and underlying symmetry, the chiral Gross-Neveu model is captured by different universality classes, referring to chiral Ising, XY and $O(3)$ universality classes[12]. More recently, it is intriguing that the Gross-Neveu model has been found to be related to the AdS/CFT theories[13].

In the case of chiral Ising universality class, the Gross-Neveu model is only renormalizable in $1 + 1$ spacetime dimensions. Another more widely studied model in this class is the GNY model [6–12, 14–25], which is renormalizable in $3 + 1$ spacetime dimensions. In contrast to the purely fermionic Gross-Neveu model, the GNY model can be rewritten by introducing an auxiliary scalar field so that the Lagrangian is quadratic in fermion field[3]. But now, the scalar field has a canonical kinetic term and the scalar field interacts quartically[12]. For its wide applica-

tions in many areas of physics ranging from high-energy physics to quantum criticality, the GNY model has been studied by a broad range of different methods, including functional renormalization group[9, 11, 26], conformal bootstrap[27–30] and $1/N$ expansion[17, 31–33]. The sign-free quantum Monte Carlo has been broadly used to study the fermionic quantum criticality of interacting Dirac fermions on lattice[10, 14, 34–38]. Finally, the $4 - \epsilon$ expansion is a suitable algorithms to facilitate higher-order calculations for fermionic criticality[15]. By now, the most accurate calculation has been carried up to four loops [12, 25].

In particular, the fermionic criticality in Dirac systems such as graphene has been extensively discussed[14, 19]. On graphene's honeycomb lattice, the low-energy gapless Dirac fermions with relativistic dispersion emerge at the two inequivalent Dirac points in the Brillouin zone. A typical quantum criticality of the interacting electrons on graphene's lattice is the transition from a semimetal to an ordered charge-density-wave which breaks sublattice symmetry[6, 10], triggered by sufficient large nearest-neighbor repulsion interaction. Another typical example on this lattice is the semimetal-antiferromagnetic transition favored by an onsite Hubbard repulsion[7, 9, 14]. Other examples can be constructed according to the ordered partner on the specific lattice [39–43]. The nature of the quantum phase transition for interacting Dirac fermions has been under debate for a long time[6, 44]. However, recent developments on the fermion-driven quantum critical point (FIQCP) suggest a second-order continuous phase transition between the semimetallic and the gapped phase [21–24, 36, 45–47]. The gapless Dirac fermions emerge as a new degrees of freedom, consequently, their quantum criticality can

*Electronic address: jzhou5@gzu.edu.cn

effectively be described by a chiral transitions appearing in different $2 + 1$ dimensional Gross-Neveu model, giving rise to the chiral universality classes[12]. Even in those system which supports cubic terms of order parameter, the strong fluctuations of gapless fermions would render the putatively first-order transition continuous, this is right the central idea of FIQCP[36, 45, 48, 49]. Based on the honeycomb lattice, the evidence for FIQCP have been proposed near the semimetal-Kekule valence-bond-solid transition[36, 45], similar scenario was also proposed in three-dimensional double-Weyl semimetals for semimetal-nodal-nematic order transition[47]. The FIQCP can be traced back to the fluctuations of gapless Dirac degrees of freedom at criticality.

Aside from the close connections with the quantum criticality from a Dirac semimetal to a symmetry broken phase, the GNY model also has connections with both supersymmetry [50–56] and emergent symmetry at criticality [57–64]. It is intriguing that the critical point possess some symmetries which absent in the original model at the microscopic level. For instance, right at the fixed point of the special GNY model in which the velocities for both massless Dirac fermions and relativistic bosons are not equal to each other, the Lorentz symmetry get restored at criticality, leading to the notation of an emergent Lorentz symmetry[66]. The emergent symmetry at criticality can be attributed to the presence of fluctuations of new degrees of freedom (gapless Dirac fermions).

In addition, the enlargement of symmetry was put forward to explain the continuous phase transition between two phases with different broken symmetries [57–64, 67–71]. It is argued that the deconfined quantum critical point, which separates the Neel and valence-bond-solid orders of spin-1/2 Heisenberg quantum antiferromagnet on square lattice, possesses an enlarged emergent symmetry [72–75]. Very recently, the similar enlarged emergent symmetry has been stressed in the Dirac system with competing orders[23, 64, 76, 77]. As pointed above, the critical properties of the transition from a semimetal to a gapped broken phase can be captured by GNY model[78–81], therefore it is believed that the GNY model is accessible to the emergent symmetry with an appropriate way[82, 83]. Indeed, on the basis of GNY model, it is stressed that the emergent symmetry is responsible for various deconfined transitions in Dirac systems[50, 62, 64, 84]. On the other hand, the GNY model also connect closely with the supersymmetry [50–54]. For example, the GNY model with 1/4 flavor of four-component fermions in the chiral Ising universality class relates to the $\mathcal{N} = 1$ supersymmetry[12], and the GNY model with 1/2 flavor of four-component fermions in the chiral XY universality class relates to the $\mathcal{N} = 2$ supersymmetry[54].

Although the quantum criticality from a semimetal to an $O(N)$ symmetry broken phase for $N \leq 3$ has achieved satisfactory understood, the impact of fermion degrees of freedom on the stability of the quantum critical point with emergent- $O(N)$ symmetry for $N \geq 4$ is

under debate[23]. For the fermionic criticality in Dirac systems, a variety of critical points with emergent symmetry have been put forward[41, 64, 67, 68], by now, however, what kinds of emergent symmetry is allowed is still unclear. Besides, whether the supersymmetric quantum critical point can emerge in the chiral emergent- $O(N)$ universality class remains unknown so far. The stability of the critical point with emergent- $O(N)$ symmetry, as far as we are aware, is partly answered in Refs.[23] and [64]. Motivated by these issues, in this paper, without asking the specific lattice model as well as the specific forms of symmetry broken orders, we study the critical structure and the emergent symmetry of the chiral GNY model with N_f flavors four-component fermions coupled strongly to an $O(N)$ scalar field. The present study has three purposes. The first is to determine the meaningful fixed point that controls the critical properties in the emergent- $O(N)$ universality class. The second is to confirm the reasonable emergent- $O(N)$ symmetry in Dirac systems. Our final purpose is to find the possible supersymmetric critical point in the chiral emergent- $O(N)$ universality class. To investigate the impact of gapless Dirac fermion degrees of freedom, we also introduce a small $O(N)$ -anisotropy that breaks $O(N)$ symmetry in the chiral GNY model.

The rest of the paper is organized as follows. We define the chiral GNY model in Sec.II. In Sec.III, we review the basic renormalization group (RG) procedure and give our results for beta functions and anomalous dimensions. In Sec.IV, we discuss the stability and the emergent symmetry for the emergent- $O(N)$ fixed point, the supersymmetric quantum critical point in the chiral emergent- $O(N)$ universality class is also discussed in this section. Finally, our conclusions and some comments are provided in Sec.V. More details for the determination of renormalization constants are presented in Appendix A.

II. THE GROSS-NEVEU-YUKAWA MODEL

We first define the chiral GNY model under investigation. As pointed in the introduction, for various interacting relativistic fermions systems in $2 + 1$ dimensions, the quantum phase transition towards a symmetry-broken phase can be captured by the chiral GNY model in which the fermions couple strongly to a multicomponent boson fields via Yukawa coupling. Formally, the general chiral $O(N)$ -GNY model in D -dimensions Euclidean spacetime can be described by the effective action

$$S = \int d^D x (\mathcal{L}_\psi + \mathcal{L}_\phi + \mathcal{L}_{\psi\phi}). \quad (1)$$

The Lagrangian for fermions is simply abbreviated as

$$\mathcal{L}_\psi = \bar{\psi}_i i \not{\partial} \psi_i, \quad (2)$$

where the notation $\not{\partial} = \gamma_\mu \partial_\mu$ is the Feynman slash, and the 4×4 gamma matrices γ_μ form a four-dimensional

representation of the Clifford algebra, i.e., $\{\gamma_\mu, \gamma_\nu\} = 2\delta_{\mu\nu}1_4$, with the indices $\mu, \nu = 0, 1, \dots, D-1$ and 1_4 denotes the identity matrix. The Dirac spinor ψ_i is a four-component fermion spinor and its conjugate is defined as $\bar{\psi}_i = \psi_i^\dagger \gamma_0$. For generality, we have introduced N_f flavors of four-component spinor such that the Dirac spinor carries a flavor index $i, i = 1, \dots, N_f$. The summation convention over repeated indices is also assumed here and in the following.

The second term in (1) describes the purely bosonic part. Explicitly, it takes the form as

$$\mathcal{L}_\phi = \frac{1}{2}(\partial_\mu \phi_a)^2 + \frac{m^2}{2}\phi_a \phi_a + \frac{\lambda_1}{4!}(\phi_a \phi_a)^2 + \frac{\lambda_2}{4!}(\phi_a)^4. \quad (3)$$

Here, the index a in ϕ_a takes the value range from 1 to N . In addition to the kinetic term and quartic interactions with strength λ_1 , a small anisotropy (with strength λ_2) that breaks $O(N)$ symmetry is added to investigate the impact of gapless Dirac fermion degrees of freedom. The mass-square m^2 plays the role of tuning parameter for phase transition, $m^2 > 0$ corresponds to symmetric phase with $\langle \phi_a \rangle = 0$, $m^2 < 0$ corresponds to symmetry broken phase and $m^2 = 0$ at criticality. In the symmetry broken ground state, the scale field ϕ_a acquires a nonzero vacuum expectation, then the fermion mass is generated dynamically. For the pure $O(N)$ scalar model, although the symmetry is broken by the small anisotropy presented in the last term, it is shown that the symmetry is restored at criticality for $N < 3$ [85, 86]. The $O(N)$ fixed point is unstable under anisotropy for $N > 3$. In this paper, we will demonstrate the impact of gapless Dirac fermion degrees of freedom on the stability of the $O(N)$ fixed point.

Finally, $\mathcal{L}_{\psi\phi}$ defines the Yukawa coupling between gapless Dirac fermions and $O(N)$ -symmetric scalar fields with strength g :

$$\mathcal{L}_{\psi\phi} = g\bar{\psi}_i [(\Sigma_a)_{4N_f \times 4N_f} \cdot \phi_a] \psi_i. \quad (4)$$

Each Σ_a signals the broken pattern of various gapped phases, their dimension depend on the specific lattice model. More precisely, the dimension for these sigma matrices coincides with the components of Dirac spinor. For example, the spinless fermions on honeycomb lattice define a four-component Grassmann spinor, the dimension for the sigma matrix is four. On the other hand, the spinful fermions on honeycomb lattice define an eight-component Dirac spinor, now the dimension for the sigma matrix is eight.

To continue the following calculation, commuting rules between these sigma matrices and Dirac gamma matrices are required. In the chiral Ising universality class for $N = 1$, the GNY model Eq.(1) includes an one-component real scalar field, Σ_1 is a trivial identity matrix in this case, so we have $[\gamma_\mu, \Sigma_1] = 0$ for chiral Ising-GNY model. In the chiral XY universality class for $N = 2$, the GNY model includes a complex order parameter, now the Yukawa term can be generally written as $\mathcal{L}_{\psi\phi} = g\bar{\psi}_i(\phi_1 + i\gamma^5\phi_2)\psi_i$, where $\{\gamma^5, \gamma_\mu\} = 0$

and the explicit choice of γ^5 depends on the specific model[20, 87, 88]. Note that $\gamma^5 S_\psi(p) = -S_\psi(p)\gamma^5$, where $S_\psi(p)$ is the fermion propagator. Since in any non-vanished Feynman loop, each fermion propagator is attached by two $i\gamma^5$ factors at both sides respectively, then the minus generated from the interchange of γ^5 and $S_\psi(p)$ is countered by $i^2 = -1$. Therefore, the vanished commutator $[\vec{\Sigma}_{XY}, \gamma_\mu] = 0$ works in the practical calculations for chiral XY-GNY model. Finally, in the chiral $O(3)$ universality class for $N = 3$, the three-component order parameters break spin-rotational symmetry spontaneously. An explicit choice of the Yukawa interactions is given in Ref.[9], and the commutator $[\vec{\Sigma}_{O(3)}, \gamma_\mu] = 0$ is satisfied.

Since the emergent $O(N)$ symmetry for $N \geq 4$ can be builded on the competing orders that break these three basic symmetries[41, 59, 64], it is reasonable to assume the commuting rules

$$[\Sigma_a, \gamma_\mu] = 0, \quad \forall a, \mu, \quad (5)$$

in chiral $O(N)$ -GNY model. This vanished commutator is essential for the derivation of fixed points and critical exponents in the chiral emergent- $O(N)$ universality class. In the practical calculation, all beta and eta functions are independent from the explicit matrix representation of the Dirac gamma matrix, and only the Clifford algebra and the dimensions of the representation matrix are required in the renormalization group calculations. At the tree level, the scaling dimensions for the field variables and coupling constants can be identified from Eq.(1),

$$[\psi] = \frac{D-1}{2}, \quad [\phi] = \frac{D-2}{2}, \quad (6)$$

$$[\lambda] = 4-D, \quad [g] = \frac{4-D}{2}. \quad (7)$$

The Yukawa coupling g , quartic $O(N)$ -interaction λ_1 , as well as the strength for small $O(N)$ -symmetry-breaking perturbations λ_2 , are all marginal at the upper critical dimension $D_{uc} = 4$, implying that the critical properties is accessible via standard epsilon expansion in $D = 4 - \epsilon$ spacetime dimensions.

III. FIELD THEORY AND RENORMALIZATION GROUP

This section present the renormalization group (RG) analysis of the chiral $O(N)$ -GNY model under a small $O(N)$ -symmetry-breaking perturbation, see Eq.(1). To perform standard RG analysis in $4 - \epsilon$ dimensions, we employ dimensional regularization and modified minimal subtraction (MS) scheme. The bare Lagrangian is defined by replacing the field variables and different couplings with their bare counterparts, i.e.,

$$\psi \rightarrow \psi_0, \phi \rightarrow \phi_0, \lambda \rightarrow \lambda_0, g \rightarrow g_0, m^2 \rightarrow m_0^2. \quad (8)$$

The renormalized Lagrangian is then written as

$$\begin{aligned} \mathcal{L} = & Z_\psi \bar{\psi}_i i \not{\partial} \psi_i + \frac{1}{2} Z_\phi (\partial_\mu \phi_a)^2 + \frac{1}{2} Z_\phi Z_{m^2} m^2 \phi_a^2 \\ & + \frac{\lambda_1}{4!} \mu^\epsilon Z_{\lambda_1} Z_\phi^2 (\phi_a \phi_a)^2 + \frac{\lambda_2}{4!} \mu^\epsilon Z_{\lambda_2} Z_\phi^2 (\phi_a)^4 \\ & + g \mu^{\epsilon/2} Z_g Z_\psi \sqrt{Z_\phi} \bar{\psi}_i (\Sigma_a \phi_a) \psi_i. \end{aligned} \quad (9)$$

where μ is the energy-scale parameterizing the RG flow of the coupling constants. These different Z -factors are named renormalization constants, which are used to absorb the divergence in the loop corrections. The wavefunction renormalization constants Z_ψ , and Z_ϕ , relate the bare and renormalized field variables upon the field rescalings $\psi_0 = \sqrt{Z_\psi} \psi$, $\phi_0 = \sqrt{Z_\phi} \phi$. Accordingly, the bare mass-square, quartic couplings, and the Yukawa coupling are related to their dimensionless partner as following,

$$m_0^2 = \mu^2 m^2 Z_{m^2}, \quad (10)$$

$$\lambda_{10} = \mu^\epsilon \lambda_1 Z_{\lambda_1}, \quad (11)$$

$$\lambda_{20} = \mu^\epsilon \lambda_2 Z_{\lambda_2}, \quad (12)$$

$$g_0 = \mu^{\epsilon/2} g Z_g. \quad (13)$$

We have also introduced the rescaling couplings

$$g \rightarrow g \mu^{\epsilon/2}, \lambda_1 \rightarrow \lambda_1 \mu^\epsilon, \lambda_2 \rightarrow \lambda_2 \mu^\epsilon, \quad (14)$$

such that different couplings in the renormalized Lagrangian are dimensionless, this lead to explicit energy-scale dependencies Lagrangian.

The RG beta functions are defined as the logarithmic derivatives with respect to μ , $\beta(X) = dX/d \ln \mu$, where $X = m^2, \lambda_1, \lambda_2, g$. These beta functions can be derived using the fact that the bare value are independent of μ . Defining the mass-square anomalous dimensions $\gamma_{m^2} = d \ln Z_{m^2} / d \ln \mu$, we find

$$\beta(m^2) = -(2 + \gamma_{m^2}) m^2. \quad (15)$$

The $\ln \mu$ derivative of Eqs. (11)-(13) give the beta function of dimensionless couplings:

$$\beta(\lambda_1) = -\epsilon \lambda_1 - \frac{1}{Z_{\lambda_1}} \frac{\partial Z_{\lambda_1}}{\partial \ln \mu} \lambda_1, \quad (16)$$

$$\beta(\lambda_2) = -\epsilon \lambda_2 - \frac{1}{Z_{\lambda_2}} \frac{\partial Z_{\lambda_2}}{\partial \ln \mu} \lambda_2, \quad (17)$$

$$\beta(g^2) = -\epsilon g^2 - \frac{2}{Z_g} \frac{\partial Z_g}{\partial \ln \mu} g^2. \quad (18)$$

Here, we have introduced the squared Yukawa coupling g^2 for notational simplicity. In terms of these RG beta functions, the inverse correlation length exponent ν^{-1} is determined by [12, 16]

$$\nu^{-1} = -\frac{d\beta(m^2)}{m^2} = 2 + \gamma_{m^2}. \quad (19)$$

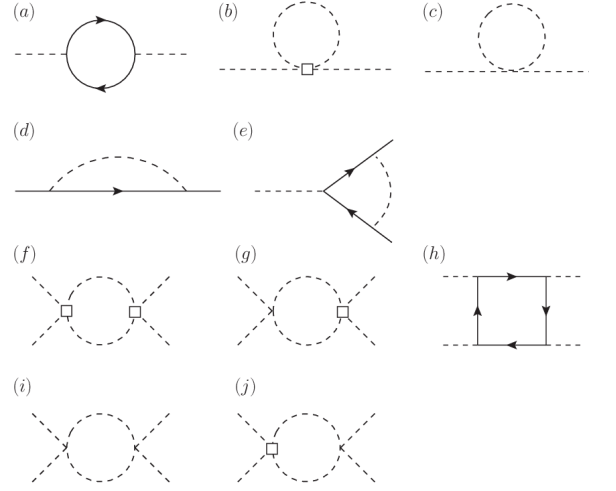


FIG. 1: One-loop 1PI diagrams. (a), (b) and (c) for boson self-energy, (d) for fermion self-energy, (e) for Yukawa vertex, (f), (g) and (h) for $O(N)$ -symmetry quartic vertex, (i) and (j) for $O(N)$ -anisotropy quartic vertex.

Furthermore, the fermion anomalous dimensions γ_ψ , and boson anomalous dimensions γ_ϕ are obtained from

$$\gamma_\phi = \frac{1}{Z_\phi} \frac{\partial Z_\phi}{\partial \ln \mu}, \quad \gamma_\psi = \frac{1}{Z_\psi} \frac{\partial Z_\psi}{\partial \ln \mu}. \quad (20)$$

Both the beta functions and anomalous dimensions can be determined from the renormalization constants in the context of the standard perturbative RG. In the next subsection, we will determine the renormalization constants at the leading order.

A. Renormalization constants

In order to access the properties of critical point, one must calculate all the renormalization constants. Using dimensional regularization and MS scheme, they depend only on the dimensionless couplings and can be expanded into the following formal Laurent series[89],

$$Z_X(1/\epsilon, \lambda_1, \lambda_2, g) = 1 + \sum_{k=1}^{\infty} Z_X^{(k)}(\lambda_1, \lambda_2, g) \frac{1}{\epsilon^k}, \quad (21)$$

which can be determined order by order in perturbative RG. To the leading order, we expand $Z_X = 1 + \delta_X$ and demand these δ_X s cancel the ultraviolet divergences of the one-loop corrections. The one-particle irreducible (1PI) diagrams for two-point boson self-energy, two-point fermion self-energy, three-point Yukawa vertex, $O(N)$ -symmetry quartic vertex, and $O(N)$ -anisotropy quartic vertex are indicated in Fig.1. To calculate these one-loop 1PI divergent diagrams, the fermion and boson propaga-

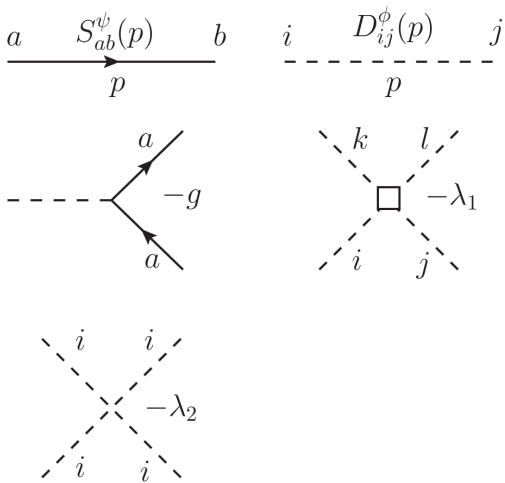


FIG. 2: Feynman rules for the fermion and boson propagators, Yukawa vertex, $O(N)$ -symmetry and $O(N)$ -anisotropy quartic vertex.

tors are

$$S_{ab}^\psi(p) = -i\delta_{ab} \frac{\not{p}}{p^2}, \quad (22)$$

$$D_{ij}^\phi(p) = \frac{\delta_{ij}}{p^2 + m^2}. \quad (23)$$

And the complete Feynman rules are illustrated in Fig.2. We present a more detailed calculations of these one-loop 1PI diagrams in Appendix A, here we only quote the final results:

$$Z_\psi = 1 - Ng^2 \frac{K}{\epsilon}, \quad (24)$$

$$Z_\phi = 1 - 4N_f g^2 \frac{K}{\epsilon}, \quad (25)$$

$$Z_{m^2} = 1 + \left(\frac{N+2}{3}\lambda_1 + \lambda_2 + 4N_f g^2\right) \frac{K}{\epsilon}, \quad (26)$$

$$Z_{\lambda_1} = 1 + \left(\frac{N+8}{3}\lambda_1 + 2\lambda_2 - 48N_f g^4/\lambda_1 + 8N_f g^2\right) \frac{K}{\epsilon}, \quad (27)$$

$$Z_{\lambda_2} = 1 + (3\lambda_2 + 4\lambda_1 + 8N_f g^2) \frac{K}{\epsilon}, \quad (28)$$

$$Z_g = 1 + (2N_f + 4 - N)g^2 \frac{K}{\epsilon}. \quad (29)$$

It is seen from above that all renormalization constants have a simple pole at ϵ . Here and in the following, the constant $K = 1/(4\pi)^2$. To derive these renormalization Z -factors, we have made use of the sigma matrix with dimensions four but without asking its explicit representation. The dimensions-dependence on the sigma matrix is generalized by introducing N_f flavors of four-component fermions.

B. Beta functions and anomalous dimensions

To derive the exact expressions of the beta functions, we first use the chain rule, to write

$$\frac{\partial Z_X}{\partial \ln \mu} = \sum_Y \frac{\partial Z_X}{\partial Y} \beta(Y), \quad (30)$$

where $X, Y \in \{m^2, \lambda_1, \lambda_2, g\}$. Inserting the renormalization Z -factors into Eqs.(16)-(18) then produces the beta functions for $O(N)$ scalar coupling λ_1 , $O(N)$ -anisotropy strength λ_2 , and squared Yukawa coupling g^2 , respectively. We find

$$\begin{aligned} \beta(\lambda_1) = & -\epsilon\lambda_1 + (N+8)K\lambda_1^2/3 + 2K\lambda_1\lambda_2 \\ & + 8KN_f g^2 \lambda_1 - 48KN_f g^4, \end{aligned} \quad (31)$$

$$\beta(\lambda_2) = -\epsilon\lambda_2 + 3K\lambda_2^2 + 4K\lambda_1\lambda_2 + 8KN_f g^2 \lambda_2, \quad (32)$$

$$\beta(g^2) = -\epsilon g^2 + (4N_f + 8 - 2N)K g^4. \quad (33)$$

Our beta function can be verified in some specific limits. For example, setting $g = 0$, we recover the one-loop beta function for the $O(N)$ scalar model under a cubic-anisotropy[90]. Setting $g = 0$ and $\lambda_2 = 0$, $\beta(\lambda_1)$ agrees exactly with the results of $O(N)$ scalar model. In the chiral GNY limit upon setting $\lambda_2 = 0$, rescaling the coupling $\alpha/8\pi^2 \mapsto \alpha$ for $\alpha = g^2$, λ_1 , λ_2 , and replacing the boson self-interactions according to $\lambda/4! \mapsto \lambda$, our beta function agrees fully with the corresponding expressions derived in the chiral GNY model [12].

In terms of Eq.(30), the inverse correlation length exponent and the anomalous dimensions [see Eqs.(19)-(20)] can be obtained, to the one-loop order, as

$$\nu^{-1} = 2 - \left(\frac{N+2}{3}\lambda_1 + \lambda_2 + 4N_f g^2\right)K. \quad (34)$$

$$\gamma_\phi = 4KN_f g^2, \quad \gamma_\psi = KN g^2. \quad (35)$$

The couplings dependence of these exponents is meant to be evaluated at the stable fixed point that controls the critical behaviors.

IV. RG ANALYSIS

We began the RG analysis by searching for the fixed points of the beta function. The beta function for the Yukawa coupling exhibits two fixed points: zero and nonzero. It is easy to see that only the fixed point with finite Yukawa value is stable, since at which the slope $\partial\beta(g^2)/\partial g^2$ is positive. In the case of $g^2 = 0$, the beta functions in Eqs.(31)-(32) admit four well understood fixed points[86, 90]: the trivial Gaussian fixed point $(0, 0)$, Ising fixed point $[\epsilon/(3K), 0]$, anisotropic fixed point $[\epsilon/(NK), (N-4)\epsilon/(3NK)]$, and isotropic Wilson-Fisher fixed point $[3\epsilon/((N+8)K), 0]$. The most intriguing fixed

points are the Wilson-Fisher and the anisotropic fixed points as they exchange their stability at the critical dimensionality $N_c \approx 3$, see for example in Ref.[86].

At the fixed point with finite Yukawa coupling, solving the common zero of Eqs.(31) and (32), we find four different fixed points: two Yukawa-Wilson-Fisher (YWF) fixed points and two fixed points with small $O(N)$ -symmetry-breaking anisotropy which we will term anisotropic fixed point (AFP). Among all those fixed points, we are interesting in the ones with positive λ_1 , so-called YWF2 fixed point and AFP2, as their stability depend on the value of N and fermion flavors N_f . The YWF2 fixed point locates at

$$\lambda_{1*} = \frac{3F + N^2 - 8N - 4N_f^2 + 16}{2(N+8)(2N_f - N + 4)^2} \frac{\epsilon}{K}, \quad (36)$$

$$\lambda_{2*} = 0, \quad (37)$$

$$g_*^2 = \frac{1}{2(2N_f - N + 4)} \frac{\epsilon}{K}, \quad (38)$$

defining

$$F \equiv \sqrt{[(N-4)^2 + 4N_f^2 + 20N_fN + 112N_f]F_0}, \quad (39)$$

with $F_0 = (2N_f - N + 4)^2$, and the AFP2 locates at

$$\lambda_{1*} = \frac{W + 2N_f + N - 4}{2N(N - 2N_f - 4)} \frac{\epsilon}{K}, \quad (40)$$

$$\lambda_{2*} = \frac{-2W + (N + 2N_f - 6)N - 4N_f + 8}{3N(N - 2N_f - 4)} \frac{\epsilon}{K}, \quad (41)$$

$$g_*^2 = \frac{1}{2(2N_f - N + 4)} \frac{\epsilon}{K}, \quad (42)$$

where $W = [4N_f^2 + 4N_f(37N - 4) + (N - 4)^2]^{1/2}$. The stable fixed point occurs at the nonzero Yukawa coupling, thus the chiral $O(N)$ universality class has strongly boson-fermion coupled critical fluctuations. We will analysis the interplay between the boson-fermion coupled critical fluctuations and the small $O(N)$ -symmetry-breaking anisotropy.

A. Stability analysis

The stability of the fixed points is determined by a matrix M_{ij} , which is termed stability matrix and defined as the first derivatives of the beta functions with respect to the couplings

$$M_{ij} = \frac{\partial \beta(\lambda_i)}{\partial \lambda_j}, \quad (43)$$

where $i, j = 1, 2, 3$ and $\lambda_3 = g^2$. The reliable conclusion about the stability of fixed point can be given by calculating the eigenvalues of the stability matrix taken at the fixed point. If the real part of the eigenvalues are all positive, the fixed point is stable and corresponds to a sink.

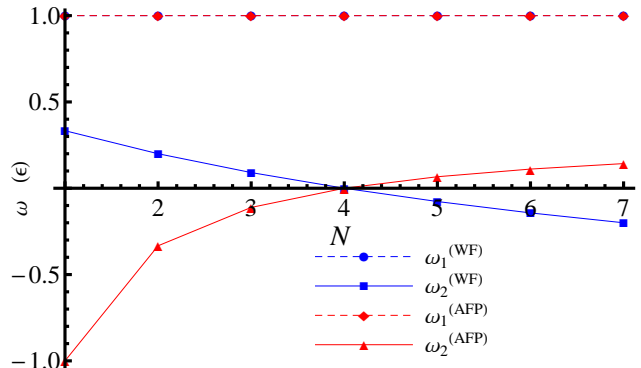


FIG. 3: Stability exponents as a function of N in the non-Yukawa limit. $\omega^{(\text{WF})}$ (blue) and $\omega^{(\text{AFP})}$ (red) denote the stability exponents evaluated at the isotropic Wilson-Fisher and the anisotropic fixed point, respectively.

On the other hand, if the real part of the eigenvalues have opposite sign, the fixed point is of a saddle-point. A saddle-point type fixed point acquires at least an unstable direction on the surface spanned by the coupling constants. An important property of the stability matrix is that its i -th eigenvalue (denoted by ω_{λ_i}) controls the RG flow approaching the fixed point along λ_i -direction. In turn, these eigenvalues are called stability exponents.

For the non-Yukawa limit with $g^2 = 0$, the stability matrix reads

$$M_{ij} = \begin{pmatrix} -\epsilon + \frac{N+8}{3} 2K\lambda_1 + 2K\lambda_2 & 2K\lambda_1 \\ 4K\lambda_2 & -\epsilon + 6K\lambda_2 + 4K\lambda_1 \end{pmatrix}.$$

To obtain the stability exponents of the fixed point, we calculate the eigenvalues of the stability matrix. The stability exponents at the isotropic Wilson-Fisher (or named Heisenberg) fixed point and the anisotropic fixed point are plotted in Fig.3, respectively. It is seen from Fig.3 that the critical value $N_c = 4$ separates two distinct regimes of the stable fixed point. For $N < N_c$, the isotropic Wilson-Fisher fixed point is stable. While for $N > N_c$, the anisotropic fixed point is stable as the stability exponents $\omega_1^{(\text{AFP})} > 0$ and $\omega_2^{(\text{AFP})} > 0$ in this regime. Therefore, both fixed points merge into a single point and exchange their stability at N_c . For the most accurate value of N_c , early four and five-loop approximations suggest it lies below 3 [85, 86].

Let us now concentrate our attentions on the YWF2 fixed point. In the presence of finite Yukawa coupling, the stability matrix can be derived from Eqs.(31)-(33). Diagonalization of the stability matrix shows that the stability of the YWF2 fixed point depends on N . In Fig.4, we plot the stability exponents of the YWF2 fixed point for $N_f = 1$ and $N_f = 2$. In the case of $N_f = 1$, the first exponents are constantly positive for different N , while the second exponent changes its sign at $N \approx 11$,

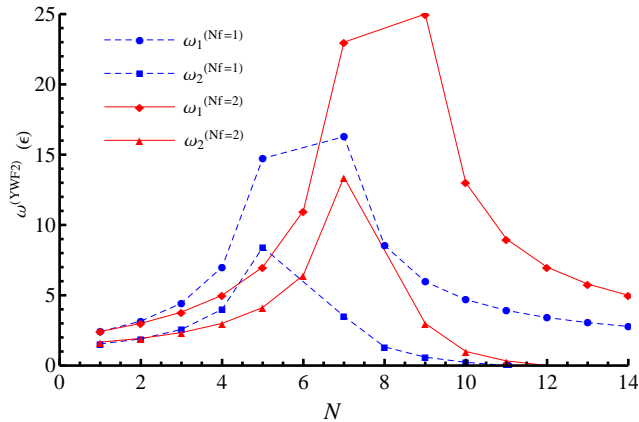


FIG. 4: Numerical results for the first two stability exponents at the YWF2 fixed point as a function of N . dashed blue line is plotted for $N_f = 1$ and red line is plotted for $N_f = 2$.

see the blue-square in Fig.4. This implies that the YWF2 fixed point is stable and governs the critical behaviors for $N < 11$. In the case of $N_f = 2$, the stability exponents are illustrated by red line in Fig.4, the results are qualitatively similar as that for $N_f = 1$ but the stability is separated by $N = 12$ (see red triangle). Further, we also determine the stability of YWF2 fixed point as the function of flavors of fermions, and the results are shown in Fig.5. From Fig.5, we see that the exponents for different N do not change their sign as N_f increases. In particular, the YWF2 fixed point in chiral emergent- $O(4)$ and $O(5)$ universality class is stable, this implies fermion-induced symmetry enhancement in interacting Dirac fermion systems[23, 64].

The stable YWF2 fixed point means that the $O(N)$ -anisotropy is irrelevant. Indeed, for $N = 1$, the initial model possesses an exchange symmetry $\lambda_1 \leftrightarrow \lambda_2$. As a result, the beta functions should obey the relation $\beta(\lambda_1 + \lambda_2) = \beta(\lambda_1) + \beta(\lambda_2)$, the anisotropic fixed point and the isotropic fixed point merge to form a new Yukawa Wilson-Fisher (stable) fixed point. Then the initial model reduce to the chiral Ising GNY model with an effective coupling $\lambda_e = \lambda_1 + \lambda_2$ in this special case.

B. RG flows

Aside from the stability analysis for the fixed point, RG flows provide us with an alternative way to investigate the properties of the fixed point. Since the beta function for Yukawa coupling is independent of λ_1 and λ_2 [see Eq.(33)], the stable fixed point shares the common Yukawa value. Therefore, it is sufficient only to plot the projected RG flows in the λ_1 - λ_2 plane at the finite Yukawa coupling.

We plot the RG flows for $N_f = 1$ in Fig.6(a)-(c). For the chiral $O(4)$ -GNY model [Fig.6(a)], the YWF2 fixed

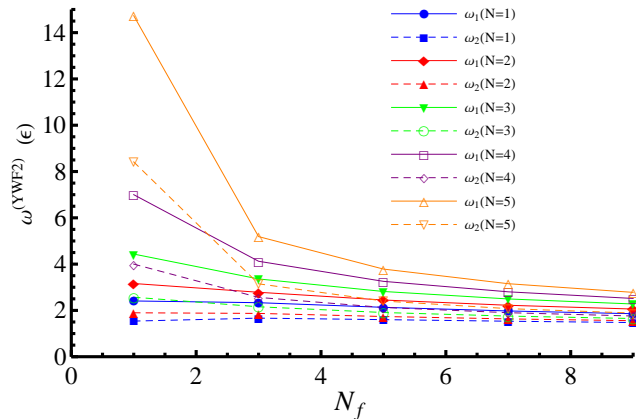


FIG. 5: Stability exponents of the YWF2 fixed point for different N as a function of N_f .

point is a stable point, while the AFP2 is a saddle point. With the increase in N , AFP2 moves gradually toward YWF2 fixed point, then they merge into a single point M at about $N = 11$, as shown in Fig.6(b). Right at the point M, the beta functions have a marginal component in λ_2 -direction. With further increase of N , the YWF2 fixed point acquires one unstable direction, and the AFP2 turns into a stable one in Fig.6(c). Further, the RG flows for $N_f = 2$ are illustrated in Fig.6(d)-(f). As in the case of $N_f = 1$, the YWF2 fixed point is stable and controls the critical behavior in the chiral $O(4)$ universality class. With the increase in N , the YWF2 fixed point and AFP2 merge into a single point M at $N = 12$. The YWF2 fixed point is stable for $N < 12$, while the AFP2 is stable for $N > 12$. These RG flows are in consistent with the stability analysis.

Although the RG flows suggest another stable fixed point (say AFP2) for sufficiently large N , what has to be emphasized is that such a new fixed point is not physically meaningful and cannot be reached in Dirac systems since the Yukawa coupling now is immeasurable for sufficiently large N [see Eq.(42)]. The non-negativity of the squared Yukawa coupling implies that N has an upper boundary. As a consequence, the emergent symmetry has a maximum value in different Dirac fermion systems.

C. Critical exponents and emergent symmetries

When the system is tuned to criticality, all couplings flow to the infrared stable fixed point at which the system exhibits scale invariance. Close enough to the scale invariant point, the correlation length and two-point correlation functions have the form of simple power-law. These power exponents define the critical exponents. Here, we calculate the inverse correlation length exponent, bosonic anomalous dimensions, and the fermionic

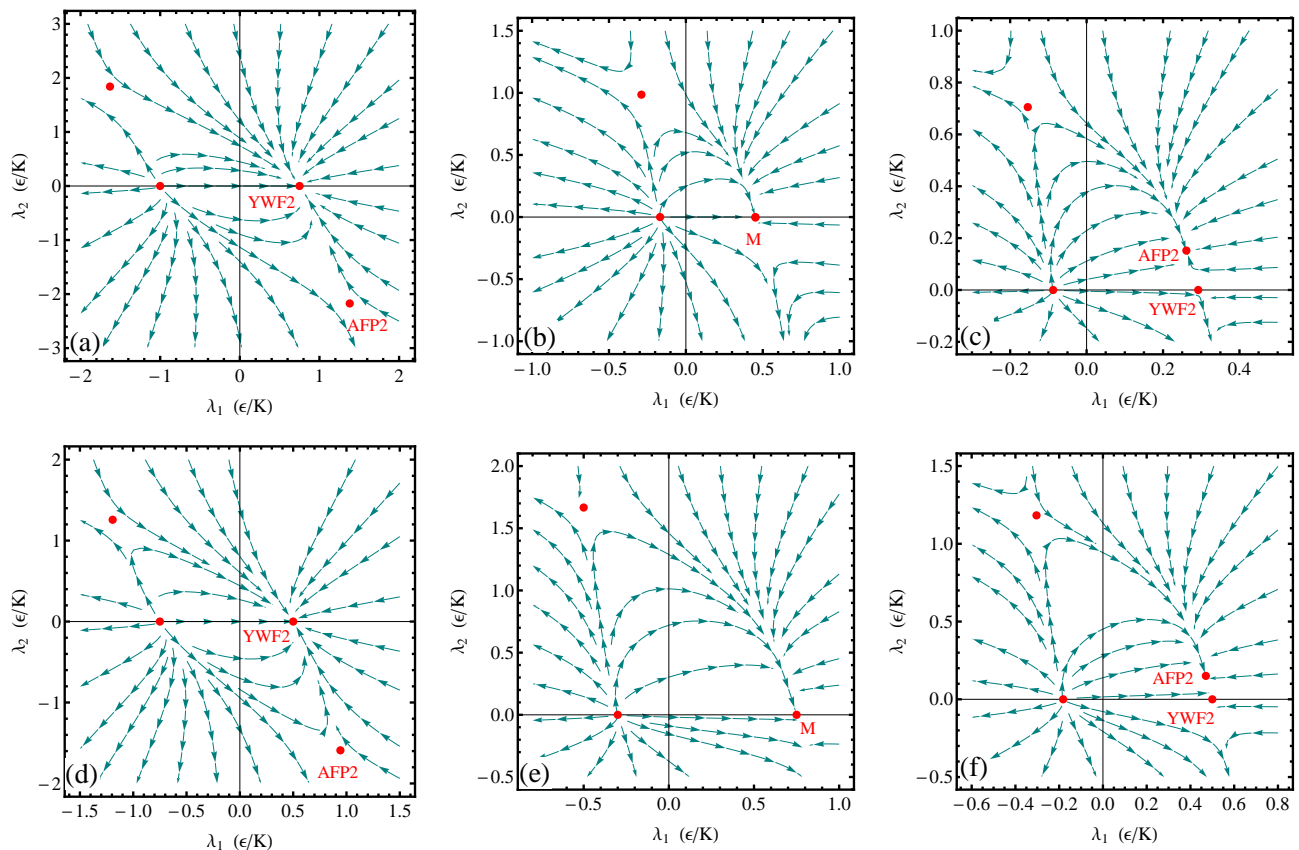


FIG. 6: Projected RG flows in the λ_1 - λ_2 plane. The first row (a)-(c) display the flows for $N_f = 1$. Panel (a) is plotted for $N = 4$, the YWF2 fixed point is stable and AFP2 is unstable. With the increase in N , two fixed points merge into a single point M at $N \approx 11$ in (b). Panel (c) is plotted for $N = 14$, the YWF2 fixed point is unstable and AFP2 is stable in (c). The second row (d)-(f) display the flows for $N_f = 2$. Panel (d) is plotted for $N = 4$, the YWF2 fixed point is stable and AFP2 is unstable. With the increase in N , two fixed points merge into a single point M at $N = 12$ in (e). Panel (f) is plotted for $N = 14$, the YWF2 fixed point is unstable and AFP2 is stable in (f).

anomalous dimensions for the chiral $O(N)$ -GNY model at the physically reasonable fixed point. Furthermore, we also discuss the supersymmetric quantum critical point in the chiral emergent- $O(N)$ universality class.

Near the stable YWF2 fixed point, the anomalous dimensions for bosons as well as fermions, to the leading order in $\epsilon = 4 - D$, read

$$(\eta_\phi, \eta_\psi) = \left[\frac{2N_f}{(2N_f - N + 4)}, \frac{N}{2(2N_f - N + 4)} \right] \epsilon, \quad (44)$$

which control the scaling of two-point boson and fermi correlation functions. Inserting the YWF2 fixed point into Eq.(34), we find for the inverse correlation length exponent

$$\frac{1}{\nu_y} = 2 - \frac{(N+2)(F+N^2-8N-4N_f^2+16)}{2(N+8)(2N_f-N+4)^2} \epsilon - \frac{2N_f}{2N_f-N+4} \epsilon. \quad (45)$$

For $N_f = 2$, the numerical evaluation of the expression provides the following series in ϵ : $\nu_y^{-1} = 2 - 0.9524\epsilon$

($N = 1$) and $\nu_y^{-1} = 2 - 1.2\epsilon$ ($N = 2$), in full agreement with the previous study in the chiral Ising and chiral XY universality class[12]. When extrapolated to $\epsilon = 1$, the anomalous dimensions [see Eq.(44)] at the linear order in ϵ must be non-negative. Then, the non-negativity of the anomalous dimensions imposes a constraint on N , or on the emergent $O(N)$ symmetry, reading

$$N < 2N_f + 4. \quad (46)$$

Meanwhile, we note that this constraint is also a natural result of the measurability of Yukawa coupling. Due to the constraint, the AFP2 is therefore a non-physical fixed point for $N_f = 1$ and $N_f = 2$.

The numerical series for the inverse correlation length exponent ν_y^{-1} have been provided in Table I. In general, the chiral $O(N)$ universality class are divided into two classes. The first class is the conventional chiral $O(N)$ universality class in which the ordered phase breaks some basic symmetries. Another class is the chiral emergent- $O(N)$ universality class in which the critical point possesses an enlargement of the basic symmetries. For instance, the chiral Ising-GNY model is relevant to

the quantum criticality of semimetal-CDW transition on graphene's honeycomb lattice, where the ordered state breaks Z_2 sublattice symmetry spontaneously. The chiral XY-GNY model has connections with superconducting or Kekulé valence-bond-solid transition in graphene, where the ordered state breaks $U(1) \simeq O(2)$ symmetry. The chiral $O(3)$ -GNY model describes the transition towards an antiferromagnetic order that breaks $SU(2)$ symmetry in related materials. These are three typical examples in the conventional chiral $O(N)$ universality class. For the chiral emergent- $O(N)$ universality class, however, it cannot be achieved by breaking a single conventional symmetry. In fact, the emergent symmetry can be realized in some special cases when two ordered phases with different broken symmetry meet at a common critical point[23, 64].

Limited by the constraint on N , the emergent- $O(N)$ symmetry depends on the number of fermion flavor and has an upper boundary $O(2N_f + 3)$. Specifically, in the Dirac system with single flavor ($N_f = 1$) of four-component fermions, the emergent- $O(4)$ and $O(5)$ symmetries at criticality are possible. And in the system with two flavors ($N_f = 2$) of four-component fermions, the emergent- $O(N)$ symmetry for $N = 4, 5, 6, 7$ are possible to be found. More importantly, since the constraint on N are obtained from the leading-order anomalous dimensions which are not affected by higher-order corrections, thus the constraint holds in any higher-order computations. What we want to emphasize in particular is that close enough to the critical point the emergent symmetry- $O(2)$ ($Z_2 \times Z_2$) and $O(3)$ ($Z_2 \times O(2)$ [64]) are also compatible with the constraint.

Finally, let us briefly discuss the emergent supersymmetric critical point. For $N_f = 1/4$, the GNY model in the chiral Ising universality class exhibits an emergent supersymmetry, the YWF2 fixed point now becomes a supersymmetric fixed point at which $\eta_\phi = \eta_\psi = \epsilon/7$. Another interesting case is the $N_f = 1/2$ GNY model in the chiral XY universality class[54], this version of model has been argued that the supersymmetry might emerges at the critical point, with the anomalous dimensions are given by $\eta_\phi = \eta_\psi = \epsilon/3$. In general, we note from Eq.(44) that the supersymmetry is ensured by $N = 4N_f$. As a result, the supersymmetry is expected to be emerged from the quantum critical point characterized by an emergent- $O(4)$ symmetry, such supersymmetric critical point is expected to be found in the chiral GNY model with single flavor ($N_f = 1$) of four-component fermions.

V. CONCLUSIONS AND COMMENTS

Within the first-order ϵ expansion, we have studied the critical structure and the emergent symmetry of chiral GNY model in the presence of a small $O(N)$ -anisotropy. This model includes a Yukawa term with N_f flavors of four-component Dirac fermions strongly coupled to an $O(N)$ scalar field. We have determined the stability of

TABLE I: Numerical series of the inverse correlation length exponent ν_y^{-1} at the stable YWF2 fixed point.

Basic $O(N)$ symmetry	$N_f = 1$	$N_f = 2$
Z_2 ($N=1$)	$2 - 0.8347\epsilon$	$2 - 0.9524\epsilon$
$O(2)$	$2 - 1.1325\epsilon$	$2 - 1.2\epsilon$
$O(3)$	$2 - 1.5988\epsilon$	$2 - 1.5273\epsilon$
Emergent $O(N)$ symmetry	$N_f = 1$	$N_f = 2$
$O(4)$	$2 - 2.5\epsilon$	$2 - 2.0\epsilon$
$O(5)$	$2 - 5.1583\epsilon$	$2 - 2.7692\epsilon$
$O(6)$	not exist	$2 - 4.2857\epsilon$
$O(7)$	not exist	$2 - 8.8\epsilon$

the fixed points and computed the critical exponents by means of perturbative renormalization in $4 - \epsilon$ dimensions. On the basis of $O(N)$ -GNY model, we have discussed the physically reasonable emergent symmetry in Dirac systems. Further, the supersymmetric quantum critical point in the emergent- $O(4)$ universality class have also been discussed briefly. The main three conclusions of our findings can be summarized as follows.

(i) The GNY model in the chiral Ising, chiral XY, or chiral $O(3)$ universality class has a unique infrared-stable fixed point, the so called Wilson-Fisher-Yukawa fixed point. For the GNY model in the chiral emergent- $O(N)$ universality class with $N \geq 4$, in order to meet the requirements of measurability for Yukawa coupling, the chiral emergent- $O(N)$ universality class is physically meaningful if and only if N is less than $2N_f + 4$, where N_f is the number of flavors of four-component Dirac fermions. On the premise that the emergent- $O(N)$ universality class is meaningful, the GNY model in the chiral emergent- $O(N)$ universality class is also dominated by the Wilson-Fisher-Yukawa fixed point. This result holds at least in the cases with $N_f = 1$ and $N_f = 2$. As a result, the small $O(N)$ -anisotropy that breaks $O(N)$ symmetry is irrelevant in the chiral emergent- $O(N)$ universality class.

(ii) The non-negativity of the anomalous dimensions and the measurability of the Yukawa coupling impose the constraint $N < 2N_f + 4$ on the emergent- $O(N)$ symmetry. As a result, the emergent symmetry has an upper boundary $O(2N_f + 3)$ in Dirac systems. The enlarged emergent- $O(4)$ and $O(5)$ symmetries are possible to be found in the system with single flavor ($N_f = 1$) of four-component fermions, and the enlarged emergent- $O(4)$, $O(5)$, $O(6)$ and $O(7)$ symmetries are expected to be found in the systems with two flavors ($N_f = 2$) of four-component fermions. These results hold in any higher-loops calculations. Moreover, the emergent- $O(2)$ ($Z_2 \times Z_2$) and $O(3)$ ($Z_2 \times O(2)$ [64]) symmetries are also compatible with the constraint.

(iii) In the chiral emergent- $O(4)$ universality class, there is a supersymmetric critical point, with the anomalous dimensions $\eta_\phi = \eta_\psi = \epsilon$. The supersymmetry is expected to be found in the system with fermion flavor $N_f = 1$.

Our result has close connections with the recent study on the quantum multicritical point that possesses enlarged emergent- $O(N)$ symmetry in Dirac systems. Refs.[23] and [64] pointed that the multicritical point between the distinct $O(s_1)$ and $O(s_2)$ symmetry broken phases is generically characterized by an emergent $O(s_1 + s_2)$ symmetry. For the conventional broken symmetries in Dirac systems, e.g., Z_2 , $O(2)$ and $O(3)$, our result agrees well with Refs.[23] and [64]. In addition, our result also suggests some rich emergent symmetries for fermionic criticality in graphene-like systems, for instance, the deconfined transition with emergent $Z_2 \times Z_2 \times O(2)$, $Z_2 \times O(2) \times O(2)$ and $O(2) \times O(2) \times O(3)$ symmetries and so on. This conjecture deserves further investigation in future. Importantly, our result is applicable to the recently observed emergent- $O(4)$ symmetry[57], the deconfined transition between $SO(3)$ -semimetal and $U(1)$ -insulator[84], or the transition between antiferromagnetism and valence-bond-solid in quantum Monte Carlo simulations of a designed synthetic Dirac systems[62].

Finally, the new emergent- $O(4)$ supersymmetric critical point is interesting on its own. In the future, we expect such supersymmetric critical point could be cross-checked by other methods, i.e., conformal bootstrap approach and quantum Monte Carlo simulation[54].

Acknowledgments

We acknowledge the support from the startup grant under No.20175788 in Guizhou University.

Appendix A: Renormalization constants at one-loop order

This appendix devotes to calculate the renormalization constants. At one-loop order, the renormalization constants are defined as $Z_X = 1 + \delta_X$, these δ_X s are known as counterterms which are used to absorb the divergencies in the 1PI diagram. Therefore, we need to calculate all the divergence of the 1PI diagrams in Fig. 1.

1. Vertex tensor product

Before the calculation, let us derive the vertex product contributing to the effective quartic boson interaction. The general vertex tensor can be represented as the following symmetrized form: $\lambda_{ijkl} = \lambda_1 T_{ijkl}^{(1)} + \lambda_2 T_{ijkl}^{(2)}$, with

$$T_{ijkl}^{(1)} = \frac{1}{3}(\delta_{ij}\delta_{kl} + \delta_{ik}\delta_{jl} + \delta_{il}\delta_{jk}), \quad (\text{A1})$$

$$T_{ijkl}^{(2)} = \delta_{ijkl} = \begin{cases} 1, & i = j = k = l, \\ 0, & \text{otherwise.} \end{cases} \quad (\text{A2})$$

Here, δ_{ijkl} satisfies $\sum_k \delta_{ijkk} = \delta_{ij}$, $\sum_i \delta_{ii} = N$. The leading order 1PI diagram for quartic boson interaction need to calculate the tensor product: $\lambda_{ijmn}\lambda_{mnlk}$. For $T^{(1)}T^{(1)}$, we have

$$T_{ijmn}^{(1)}T_{mnlk}^{(1)} = \frac{1}{9}[(N+4)\delta_{ij}\delta_{kl} + 2\delta_{ik}\delta_{jl} + 2\delta_{il}\delta_{jk}]. \quad (\text{A3})$$

After symmetrization, we have the symmetrized result

$$\left[T_{ijmn}^{(1)}T_{mnlk}^{(1)} \right]_s = \frac{N+8}{9}T_{ijkl}^{(1)}. \quad (\text{A4})$$

Accordingly,

$$\left[T_{ijmn}^{(1)}T_{mnlk}^{(2)} + T_{ijmn}^{(2)}T_{mnlk}^{(1)} \right]_s = \frac{2}{3}T_{ijkl}^{(1)} + \frac{4}{3}T_{ijkl}^{(2)}, \quad (\text{A5})$$

$$\left[T_{ijmn}^{(2)}T_{mnlk}^{(2)} \right]_s = T_{ijkl}^{(2)}. \quad (\text{A6})$$

Combining the above results together, the symmetrized tensor product is given by

$$\begin{aligned} [\lambda_{ijmn}\lambda_{mnlk}]_s &= \left[\frac{N+8}{9}\lambda_1^2 + \frac{2\lambda_1\lambda_2}{3} \right] T_{ijkl}^{(1)} \\ &+ \left[\lambda_2^2 + \frac{4\lambda_1\lambda_2}{3} \right] T_{ijkl}^{(2)}. \end{aligned} \quad (\text{A7})$$

Finally, the product $T_{ijmn}^{(1)}\delta_{mn} = (N+2)\delta_{ij}/3$ will be necessary for boson mass-squared renormalization factor.

2. Boson two-point function

The 1PI boson two-point function are given in Fig.1(a)-(c). Fig.1(a) contributes to Z_ϕ , (b) and (c) contribute to the mass-square renormalization Z_{m^2} . Fig.1(a) gives

$$\begin{aligned} \mathcal{A}_{1a}(p) &= (-1)(-g)^2 N_f \int \frac{d^d k}{(2\pi)^d} \text{Tr} \left[\Sigma_a \frac{1}{i\cancel{k}} \Sigma_b \frac{1}{i(\cancel{k} + \cancel{p})} \right] \\ &= g^2 N_f D_\Sigma \delta_{ab} \int \frac{d^d k}{(2\pi)^d} \left[\frac{1}{\cancel{k}} \frac{1}{(\cancel{k} + \cancel{p})} \right]. \end{aligned} \quad (\text{A8})$$

where the minus sign (-1) arises from fermion loop. The integral is a standard Feynman integral, introduce a Feynman parameter and perform the elementary integral, then we have

$$\mathcal{A}_{1a}(p) = -g^2 N_f D_\Sigma \frac{K}{\epsilon} \delta_{ab} p^2, \quad (\text{A9})$$

where D_Σ is the dimensions of Σ_a , $K = 1/(4\pi)^2$ here and after in this paper. To reach the final result, the commutating rule $[\Sigma_a, \gamma_\mu] = 0$ has been used [see Eq.(5)]. We only extract the divergences when $d \rightarrow 4$ since only the divergent part should cancel out with the Z -factors, that is, these Z -factors depend only on the divergences in the dimensional regularization and MS scheme.

For Fig.1(b) and (c), we have

$$\begin{aligned}\mathcal{A}_{1b} + \mathcal{A}_{1c} &= \frac{1}{2}(-\lambda_1 T_{ijkl}^{(1)} - \lambda_2 T_{ijkl}^{(2)}) \int \frac{d^d k}{(2\pi)^d} \frac{i\delta^{kl}}{k^2 + m^2} \\ &= \left[\frac{(N+2)}{3} \lambda_1 + \lambda_2 \right] m^2 \frac{K}{\epsilon} \delta^{ij}.\end{aligned}\quad (\text{A10})$$

To reach the final result, we have used the useful integral in d -dimensional Euclidean space:

$$\int \frac{d^d k}{(2\pi)^d} \frac{1}{(k_E^2 + \Delta)^n} = \frac{1}{(4\pi)^{d/2}} \frac{\Gamma(2-d/2)}{\Gamma(n)} \frac{1}{\Delta^{2-d/2}}.\quad (\text{A11})$$

In terms of the renormalization condition

$$\mathcal{A}_{1a} + \mathcal{A}_{1b} + \mathcal{A}_{1c} - p^2 \delta_\phi - (\delta_\phi + \delta_{m^2}) m^2 = 0,\quad (\text{A12})$$

we find

$$Z_\phi = 1 - g^2 N_f D_\Sigma \frac{K}{\epsilon},\quad (\text{A13})$$

$$Z_{m^2} = 1 + \left[\frac{(N+2)}{3} \lambda_1 + \lambda_2 + g^2 N_f D_\Sigma \right] \frac{K}{\epsilon}.\quad (\text{A14})$$

3. Fermion two-point function

Fig.1(d) shows the 1PI fermion two-point function, which is given by

$$\mathcal{A}_{1d}(p) = (-g)^2 \int \frac{d^d k}{(2\pi)^d} \Sigma_a \frac{-i\cancel{k}}{k^2} \Sigma_b \frac{\delta_{ab}}{(p-k)^2 + m^2}.$$

Using the feynman parameter integral:

$$\frac{1}{k^2} \frac{1}{(p-k)^2 + m^2} = \int_0^1 dx \frac{1}{[(k+p(x-1))^2 + \Delta]^2},$$

where $\Delta = p^2 x(1-x) + m^2(1-x)$, then shifting the integration variable, $k \rightarrow k - p(x-1)$, applying the result in Eq.(A11), one obtains

$$\begin{aligned}\mathcal{A}_{1d} &= g^2 N (-i) \int_0^1 dx \int \frac{d^d k}{(2\pi)^d} \frac{-\cancel{p}(x-1)}{(k^2 + \Delta)^2}, \\ &= -g^2 N \frac{K}{\epsilon} i\cancel{p}.\end{aligned}\quad (\text{A15})$$

The divergence in Fig.1(d) should cancel out with δ_ψ , the renormalization condition is $-i\cancel{p}\delta_\psi + \mathcal{A}_{1d}(p) = 0$, we thus obtain

$$Z_\psi = 1 - g^2 N \frac{K}{\epsilon}.\quad (\text{A16})$$

4. Yukawa vertex

To the one-loop, there is a single diagram for the 1PI Yukawa vertex, see Fig.1(e). It can be calculated to give

$$\begin{aligned}\mathcal{A}_{1d}(p, q) &= \int \frac{d^d k}{(2\pi)^d} \frac{\delta_{ac}}{(p-k)^2 + m^2} \times \\ &\left[(-g\Sigma_a) \frac{1}{i(\cancel{q} + \cancel{k})} (-g\Sigma_b) \frac{1}{i\cancel{k}} (-g\Sigma_c) \right].\end{aligned}$$

The divergent part can be obtained by setting the external momentum p, q to be zero. Making use of the general Feynman parameters:

$$\frac{1}{AB^n} = \int_0^1 dx dy \delta(x+y-1) \frac{ny^{n-1}}{(xA+yB)^{n+1}},\quad (\text{A17})$$

we have

$$\begin{aligned}\mathcal{A}_{1d}(0, 0) &= g^3 \Sigma_b (2-N) \int \frac{d^d k}{(2\pi)^d} \frac{1}{k^2 + m^2} \frac{1}{k^2} \\ &= g^3 (2-N) \Sigma_b \int_0^1 dx \int \frac{d^d k}{(2\pi)^d} \frac{1}{(k^2 + xm^2)^2} \\ &= g^3 2(2-N) \Sigma_b \frac{K}{\epsilon}.\end{aligned}\quad (\text{A18})$$

The divergences should cancel out with $Z_g Z_\psi \sqrt{Z_\phi} - 1$, so, it is sufficient to define the renormalization condition

$$-g \Sigma_b (Z_g Z_\psi \sqrt{Z_\phi} - 1) + \mathcal{A}_{1d}(0, 0) = 0.\quad (\text{A19})$$

Inserting Z_ψ, Z_ϕ into it leads to

$$Z_g = 1 + g^2 [(4-N + N_f D_\Sigma/2)] \frac{K}{\epsilon}.\quad (\text{A20})$$

5. $O(N)$ -symmetric bosonic quartic-vertex

The relevant diagrams for $O(N)$ bosonic quartic-vertex are given in Fig.1(f)-(h). Fig.1(f) and (g) contribute partly to the boson self-interaction λ_1 [see Eq.(A7)], the result can be evaluated to give

$$\begin{aligned}\mathcal{A}_{1f}^{(1)} + \mathcal{A}_{1g}^{(1)} &= \frac{3}{2} [\lambda_{ijmn} \lambda_{mnkl}]_s^{(1)} \int \frac{d^d k}{(2\pi)^d} \left[\frac{1}{k^2 + m^2} \right]^2 \\ &= 3 \left[\frac{N+8}{9} \lambda_1^2 + \frac{2\lambda_1 \lambda_2}{3} \right] T_{ijkl}^{(1)} \frac{K}{\epsilon},\end{aligned}\quad (\text{A21})$$

where the number 3 counts s -channel, t -channel and u -channel in all. We have set all external momentum to be zero to get the divergences.

For Fig.1(h) with the external momentum $p = 0$, we have

$$\begin{aligned}\mathcal{A}_{1h}^{(1)}(0) &= -2N_f g^4 \int \frac{d^d k}{(2\pi)^d} \text{Tr} \left[\Sigma_i \frac{1}{i\cancel{k}} \Sigma_j \frac{1}{i\cancel{k}} \Sigma_k \frac{1}{i\cancel{k}} \Sigma_l \frac{1}{i\cancel{k}} \right] \\ &= -2N_f g^4 \int \frac{d^d k}{(2\pi)^d} \frac{1}{k^4} \text{Tr} [\Sigma_i \Sigma_j \Sigma_k \Sigma_l],\end{aligned}\quad (\text{A22})$$

where $\text{Tr}[\dots]$ in the first line denotes the trace over the sigma matrix, the number 2 in the first line counts the exchange of i and j (or equivalently, k and l). Using the identity

$$\text{Tr} [\Sigma_i \Sigma_j \Sigma_k \Sigma_l] = D_\Sigma (\delta_{ij} \delta_{kl} - \delta_{ik} \delta_{jl} + \delta_{il} \delta_{jk}),\quad (\text{A23})$$

and performing the k integration, we obtain

$$\mathcal{A}_{1h}^{(1)}(0) = -12N_f D_\Sigma g^4 \frac{K}{\epsilon} T_{ijkl}^{(1)}.\quad (\text{A24})$$

To extract the renormalization constant Z_{λ_1} , we define the renormalization condition

$$-\lambda_1(Z_{\lambda_1}Z_\phi^2 - 1)T_{ijkl}^{(1)} + \mathcal{A}_{1f}^{(1)} + \mathcal{A}_{1g}^{(1)} + \mathcal{A}_{1h}^{(1)}(0) = 0, \quad (\text{A25})$$

Inserting Z_ϕ into this condition leads to

$$Z_{\lambda_1} = 1 + \left[\frac{N+8}{3}\lambda_1 + 2\lambda_2 - 12D_\Sigma N_f g^4 / \lambda_1 + 2N_f D_\Sigma g^2 \right] \frac{K}{\epsilon}. \quad (\text{A26})$$

6. $O(N)$ -anisotropy

The diagrams for $O(N)$ -anisotropy are given in Fig.1(i) and (j), and the divergence can be computed to give

$$\begin{aligned} \mathcal{A}_{1i}^{(2)} + \mathcal{A}_{1j}^{(2)} &= \frac{3}{2} [\lambda_{ijmn} \lambda_{mnkl}]_s^{(2)} \int \frac{d^d k}{(2\pi)^d} \left[\frac{1}{k^2 + m^2} \right]^2 \\ &= 3 \left[\lambda_2^2 + \frac{4\lambda_1 \lambda_2}{3} \right] T_{ijkl}^{(2)} \frac{K}{\epsilon}. \end{aligned} \quad (\text{A27})$$

Here, to reach the final result, we have used the symmetrized tensor product Eq.(A7). Defining the renormalization condition

$$-\lambda_2(Z_{\lambda_2}Z_\phi^2 - 1)T_{ijkl}^{(2)} + \mathcal{A}_{1i}^{(2)} + \mathcal{A}_{1j}^{(2)} = 0, \quad (\text{A28})$$

and inserting Z_ϕ into it, we have

$$Z_{\lambda_2} = 1 + [3\lambda_2 + 4\lambda_1 + 2N_f D_\Sigma g^2] \frac{K}{\epsilon}. \quad (\text{A29})$$

Making use of the sigma matrix with dimensions four but without asking their explicit representation, we obtain all the renormalization constants of the main text.

-
- [1] D. Gross and A. Neveu, Dynamical Symmetry Breaking in Asymptotically Free Field Theories, *Phys. Rev. D* **10**, 3235 (1974).
 - [2] J. A. Gracey, T. Luthe, Y. Schroder, Four loop renormalization of the Gross-Neveu model, *Phys. Rev. D* **94**, 125028 (2016).
 - [3] S. Hands, A. Kocic and J. B. Kogut, Four fermion theory in fewer than four dimensions, arXiv:9208022.
 - [4] J. A. Gracey, Large N critical exponents for the chiral Heisenberg Gross-Neveu universality class, *Phys. Rev. D* **97**, 105009 (2018).
 - [5] S. Sorella, Y. Otsuka, and S. Yunoki, Absence of a Spin Liquid Phase in the Hubbard Model on the Honeycomb Lattice, *Sci. Rep.* **2**, 992 (2012).
 - [6] I. F. Herbut, Interactions and Phase Transitions on Graphene Honeycomb Lattice, *Phys. Rev. Lett.* **97**, 146401 (2006).
 - [7] F. F. Assaad and I. F. Herbut, Pinning the Order: The Nature of Quantum Criticality in the Hubbard Model on Honeycomb Lattice, *Phys. Rev. X* **3**, 031010 (2013).
 - [8] I. F. Herbut, V. Juricic, and O. Vafek, *Phys. Rev. B* **80**, 075432 (2009).
 - [9] L. Janssen and I. F. Herbut, Antiferromagnetic critical point on graphene honeycomb lattice: A functional renormalization group approach, *Phys. Rev. B* **89**, 205403 (2014).
 - [10] S. Chandrasekharan and A. Li, Quantum Critical Behavior in Three Dimensional Lattice Gross-Neveu Models, *Phys. Rev. D* **88**, 021701(R) (2013).
 - [11] B. Knorr, Critical chiral Heisenberg model with the functional renormalization group, *Phys. Rev. B* **97**, 075129 (2018).
 - [12] N. Zerf, L. N. Mihaila, P. Marquard, I. F. Herbut, and M. M. Scherer, Four-loop critical exponents for the Gross-Neveu-Yukawa models, *Phys. Rev. D* **96**, 096010 (2017).
 - [13] S. Giombi, TASI Lectures on the Higher Spin-CFT duality, arXiv:1607.02967.
 - [14] Y. Otsuka, S. Yunoki, and S. Sorella, Universal Quantum Criticality in the Metal-Insulator Transition of Two-Dimensional Interacting Dirac Electrons, *Phys. Rev. X* **6**, 011029 (2016).
 - [15] B. Rosenstein, H. L. Yu, and A. Kovner, Critical exponents of new universality classes, *Phys. Lett. B* **314**, 381 (1993).
 - [16] L. N. Mihaila, N. Zerf, B. Ihrig, I. F. Herbut, and M. M. Scherer, Gross-Neveu-Yukawa model at three loops and Ising critical behavior of Dirac systems, *Phys. Rev. B* **96**, 165133 (2017).
 - [17] J. A. Gracey, Critical exponent ω in the Gross-Neveu-Yukawa model at $O(1/N)$, *Phys. Rev. D* **96**, 065015 (2017).
 - [18] T. C. Lang and A. M. Lauchli, Quantum Monte Carlo Simulation of the Chiral Heisenberg Gross-Neveu-Yukawa Phase Transition with a Single Dirac Cone, *Phys. Rev. Lett.* **123**, 137602 (2019).
 - [19] I. F. Herbut, V. Juricic, and B. Roy, Theory of interacting electrons on the honeycomb lattice, *Phys. Rev. B* **79**, 085116 (2009).
 - [20] B. Roy, V. Juricic, and Igor F. Herbut, Quantum superconducting criticality in graphene and topological insulators, *Phys. Rev. B* **87**, 041401(R) (2013).
 - [21] M. M. Scherer and I. F. Herbut, Gauge-field-assisted Kekule quantum criticality, *Phys. Rev. B* **94**, 205136 (2016).
 - [22] Emilio Torres, Lukas Weber, Lukas Janssen, Stefan Wessel, and Michael M. Scherer, Emergent symmetries and coexisting orders in Dirac fermion systems, *Phys. Rev. Res.* **2**, 022005(R) (2020).
 - [23] Lukas Janssen, Igor F. Herbut, and Michael M. Scherer, Compatible orders and fermion-induced emergent-

- symmetry in Dirac systems, *Phys. Rev. B* **97**, 041117(R) (2018).
- [24] E. Torres, L. Classen, I. F. Herbut, and M. M. Scherer, Fermion-induced quantum criticality with two length scales in Dirac systems, *Phys. Rev. B* **97**, 125137 (2018).
- [25] B. Ihrig, L. N. Mihaila, and M. M. Scherer, Critical behavior of Dirac fermions from perturbative renormalization, *Phys. Rev. B* **98**, 125109 (2018).
- [26] H. Gies, T. Hellwig, A. Wipf, and O. Zanusso, A functional perspective on emergent supersymmetry, *J. High Energy Phys.* 12 (2017) 132.
- [27] L. Iliesiu, F. Kos, D. Poland, S. S. Pufu, D. Simmons-Duffin and R. Yacoby, Bootstrapping 3D fermions, *J. High Energy Phys.* 03 (2016) 120.
- [28] L. Iliesiu, F. Kos, D. Poland, S. S. Pufu, and D. Simmons-Duffin, Bootstrapping 3D fermions with global symmetries, *J. High Energy Phys.* 01 (2018) 036.
- [29] N. Bobev, S. El-Showk, D. Mazac, and M. F. Paulos, Bootstrapping the Three-Dimensional Supersymmetric Ising Model, *Phys. Rev. Lett.* **115**, 051601 (2015).
- [30] D. Bashkirov, Bootstrapping the $N = 1$ SCFT in three dimensions, arXiv:1310.8255.
- [31] A. N. Manashov and M. Strohmaier, Correction exponents in the Gross-Neveu-Yukawa model at $1/N^2$, *Eur. Phys. J. C* **78**, 454 (2018).
- [32] J. A. Gracey, Calculation of exponent η to $O(1/N^2)$ in the $O(N)$ Gross-Neveu model, *Int. J. Mod. Phys. A* **6**, 395 (1991). [Erratum: *Int. J. Mod. Phys. A* **6**, 2755 (1991)].
- [33] J. A. Gracey, Anomalous mass dimension at $O(1/N^2)$ in the $O(N)$ Gross-Neveu model, *Phys. Lett. B* **297**, 293 (1992).
- [34] E. Huffman and S. Chandrasekharan, Fermion bag approach to Hamiltonian lattice field theories in continuous time, *Phys. Rev. D* **96**, 114502 (2017).
- [35] Z. X. Li, Y. F. Jiang, and H. Yao, Fermion-sign-free Majorana-quantum-Monte-Carlo studies of quantum critical phenomena of Dirac fermions in two dimensions, *New J. Phys.* **17**, 085003 (2015).
- [36] Z. X. Li, Y. F. Jiang, S. K. Jian, and H. Yao, Fermion-induced quantum critical points, *Nat. Commun.* **8**, 314 (2017).
- [37] Y. Otsuka, K. Seki, S. Sorella, and S. Yunoki, Quantum criticality in the metal-superconductor transition of interacting Dirac fermions on a triangular lattice, *Phys. Rev. B* **98**, 035126 (2018).
- [38] L. Wang, P. Corboz, and M. Troyer, Fermionic quantum critical point of spinless fermions on a honeycomb lattice, *New J. Phys.* **16**, 103008 (2014).
- [39] Y. Otsuka and Y. Hatsugai, Mott Transition in the Two Dimensional Flux Phase, *Phys. Rev. B* **65**, 073101 (2002).
- [40] S. Raghu, X. L. Qi, C. Honerkamp, and S.-C. Zhang, Topological Mott Insulators, *Phys. Rev. Lett.* **100**, 156401 (2008).
- [41] S. Ryu, C. Mudry, C. Y. Hou, and C. Chamon, Masses in graphenelike two-dimensional electronic systems: Topological defects in order parameters and their fractional exchange statistics, *Phys. Rev. B* **80**, 205319 (2009).
- [42] C.Y. Hou, C. Chamon, and C. Mudry, Electron Fractionalization in Two-Dimensional Graphenelike Structures, *Phys. Rev. Lett.* **98**, 186809 (2007).
- [43] B. Roy and V. Juricic, Fermionic multicriticality near Kekule-valence-bond ordering on a honeycomb lattice, *Phys. Rev. B* **99**, 241103 (2019).
- [44] S. Sorella and E. Tosatti, Semi-metal-insulator transition of the Hubbard model in the honeycomb lattice, *Europhys. Lett.* **19**, 699 (1992).
- [45] L. Classen, I. F. Herbut, and M. M. Scherer, Fluctuation-induced continuous transition and quantum criticality in Dirac semimetals, *Phys. Rev. B* **96**, 115132 (2017).
- [46] S. K. Jian and H. Yao, Fermion-induced quantum critical points in two-dimensional Dirac semimetals, *Phys. Rev. B* **96**, 195162 (2017).
- [47] S. K. Jian and H. Yao, Fermion-induced quantum critical points in three-dimensional Weyl semimetals, *Phys. Rev. B* **96**, 155112 (2017).
- [48] S. Yin, S. K. Jian, and H. Yao, Chiral Tricritical Point: A New Universality Class in Dirac Systems, *Phys. Rev. Lett.* **120**, 215702 (2018).
- [49] S. Yin and Z. Y. Zuo, Fermion-induced quantum critical point in the Landau-Devonshire model, *Phys. Rev. B* **101**, 155136 (2020).
- [50] T. Grover, D. N. Sheng, and A. Vishwanath, Emergent Space-Time Supersymmetry at the Boundary of a Topological Phase, *Science* **344**, 280 (2014).
- [51] S. S. Lee, Emergence of supersymmetry at a critical point of a lattice model, *Phys. Rev. B* **76**, 075103 (2007).
- [52] P. Ponte and S.-S. Lee, Emergence of supersymmetry on the surface of three-dimensional topological insulators, *New J. Phys.* **16**, 013044 (2014).
- [53] S. K. Jian, Y. F. Jiang, and H. Yao, Emergent Spacetime Supersymmetry in 3D Weyl Semimetals and 2D Dirac Semimetals, *Phys. Rev. Lett.* **114**, 237001 (2015).
- [54] Z. X. Li, A. Vaezi, C. B. Mendl, and H. Yao, Numerical observation of emergent spacetime supersymmetry at quantum criticality, *Sci. Adv.* **4**, eaau1463 (2018).
- [55] W. Witczak-Krempa and J. Maciejko, Optical Conductivity of Topological Surface States with Emergent Supersymmetry, *Phys. Rev. Lett.* **116**, 100402 (2016).
- [56] A. Rahmani, X. Zhu, M. Franz, and I. Affleck, Emergent Supersymmetry from Strongly Interacting Majorana Zero Modes, *Phys. Rev. Lett.* **115**, 166401 (2015).
- [57] T. Sato, M. Hohenadler, and F. F. Assaad, Dirac Fermions with Competing Orders: Non-Landau Transition with Emergent Symmetry, *Phys. Rev. Lett.* **119**, 197203 (2017).
- [58] T. Senthil and M. P. A. Fisher, Competing orders, nonlinear sigma models, and topological terms in quantum magnets, *Phys. Rev. B* **74**, 064405 (2006).
- [59] T. Grover, T. Senthil, Topological spin hall states, charged skyrmions, and superconductivity in two dimensions. *Phys. Rev. Lett.* **100**, 156804 (2008).
- [60] A. Tanaka, and X. Hu, Many-body spin berry phases emerging from the π -flux state: competition between antiferromagnetism and the valence-bond-solid state. *Phys. Rev. Lett.* **95**, 036402 (2005).
- [61] A. Nahum, P. Serna, J. T. Chalker, M. Ortuno, and A. M. Somoza, Emergent SO(5) Symmetry at the Neel to Valence-Bond-Solid Transition, *Phys. Rev. Lett.* **115**, 267203 (2015).
- [62] Z. X. Li, S. K. Jian, and H. Yao, Deconfined quantum criticality and emergent SO(5) symmetry in fermionic systems, arXiv:1904.10975.
- [63] G. J. Sreejith, S. Powell, and A. Nahum, Emergent SO(5) Symmetry at the Columnar Ordering Transition in the Classical Cubic Dimer Model, *Phys. Rev. Lett.* **122**, 080601 (2019).
- [64] B. Roy, P. Goswami, and V. Juricic, Itinerant quantum

- multi-criticality of two dimensional Dirac fermions, Phys. Rev. B **97**, 205117 (2018).
- [65] Y. Liu, Z. Wang, T. Sato, M. Hohenadler, C. Wang, W. Guo, and F. F. Assaad, Superconductivity from the condensation of topological defects in a quantum spin-Hall insulator, Nat. Commun. **10**, 1 (2019).
- [66] B. Roy, V. Juricic and I. F. Herbut, Emergent Lorentz symmetry near fermionic quantum critical points in two and three dimensions, J. High Energy Phys. **04** (2016) 018.
- [67] S. Pujari, K. Damle, and F. Alet, Neel State to Valence-Bond-Solid Transition on the Honeycomb Lattice: Evidence for Decofined Criticality, Phys. Rev. Lett. **111**, 087203 (2013).
- [68] B. Roy and V. Juricic, Fermionic multicriticality near Kekule valence-bond ordering on a honeycomb lattice, Phys. Rev. B **99**, 241103 (2019).
- [69] A. W. Sandvik, Evidence for deconfined quantum criticality in a two-dimensional heisenberg model with four-spin interactions, Phys. Rev. Lett. **98**, 227202 (2007).
- [70] A. W. Sandvik, Continuous quantum phase transition between an antiferromagnet and a valence-bond solid in two dimensions: evidence for logarithmic corrections to scaling, Phys. Rev. Lett. **104**, 177201 (2010).
- [71] X. F. Zhang, Y. C. He, S. Eggert, R. Moessner, and F. Pollmann, Continuous Easy-Plane Decofined Phase Transition on the Kagome Lattice, Phys. Rev. Lett. **120**, 115702 (2018).
- [72] T. Senthil, A. Vishwanath, L. Balents, S. Sachdev, and M. P. A. Fisher, Decofined quantum critical points, Science **303**, 1490 (2004).
- [73] T. Senthil, L. Balents, S. Sachdev, A. Vishwanath, and M. P. A. Fisher, Quantum criticality beyond the Landau-Ginzburg-Wilson paradigm, Phys. Rev. B **70**, 144407 (2004).
- [74] Y. Q. Qin, Y. Y. He, Y. Z. You, Z. Y. Lu, A. Sen, A. W. Sandvik, C. Xu, and Z. Y. Meng, Duality between the Decofined Quantum-Critical Point and the Bosonic Topological Transition, Phys. Rev. X **7**, 031052 (2017).
- [75] C. Wang, A. Nahum, M. A. Metlitski, C. Xu, and T. Senthil, Decofined Quantum Critical Points: Symmetries and Dualities, Phys. Rev. X **7**, 031051 (2017).
- [76] J. Zhou, Y. J. Wu, and S. P. Kou, Quantum critical duality in two-dimensional Dirac semimetals, Chin. Phys. B **28** 017402 (2019).
- [77] P. Ghaemi, and S. Ryu, Competing orders in the Dirac-like electronic structure and the nonlinear sigma model with a topological term, Phys. Rev. B **85**, 075111 (2012).
- [78] X. Y. Xu and T. Grover, Competing Nodal d-Wave Superconductivity and Antiferromagnetism, Phys. Rev. Lett. **126**, 217002 (2021).
- [79] Y. Liu, W. Wang, K. Sun, and Z. Y. Meng, Designer monte carlo simulation for the gross-neveu-yukawa transition, Phys. Rev. B **101**, 064308 (2020).
- [80] Y. Liu, Z. Wang, T. Sato, W. Guo, and F. F. Assaad, Gross-Neveu Heisenberg criticality: Dynamical generation of quantum spin Hall masses, Phys. Rev. B **104**, 035107 (2021).
- [81] U. F.P. Seifert, X. Y. Dong, S. Chulliparambil, M. Vojta, H.-H. Tu, and L. Janssen, Fractionalized Fermionic Quantum Criticality in Spin-Orbital Mott Insulators, Phys. Rev. Lett. **125**, 257202 (2020).
- [82] L. Classen, I. F. Herbut, L. Janssen, and M. M. Scherer, Mott multicriticality of Dirac electrons in graphene, Phys. Rev. B **92**, 035429 (2015).
- [83] B. Roy, Multicritical behavior of $Z_2 \times O(2)$ Gross-Neveu-Yukawa theory in graphene Phys. Rev. B **84**, 113404 (2011).
- [84] Z. H. Liu, M. Vojta, F. F. Assaad, and L. Janssen, Metallic and Decofined Quantum Criticality in Dirac Systems, Phys. Rev. Lett. **128**, 087201, (2022).
- [85] H. Kleinert, S. Thoms, and V. Schulte-Frohlinde, Stability of a three-dimensional cubic fixed point in the two-coupling-constant ϕ^4 theory, Phys. Rev. B **56**, 22 (1997).
- [86] K. B. Varnashev, Stability of a cubic fixed point in three dimensions: Critical exponents for generic N , Phys. Rev. B **6**, 21 (1997).
- [87] N. Zerf, R. Boyack, P. Marquard, J. A. Gracey, and J. Maciejko, Critical properties of the valence-bond-solid transition in lattice quantum electrodynamics, Phys. Rev. D **101**, 094505 (2020).
- [88] L. Janssen, W. Wang, M. M. Scherer, Z. Y. Meng, and X. Y. Xu, Confinement transition in the QED3-Gross-Neveu-XY universality class, Phys. Rev. B **101**, 235118 (2020).
- [89] M. E. Peskin and D. V. Schroeder, An Introduction to Quantum Field Theory, Perseus, Reading MA, 1995.
- [90] D. J. Amit, Field theory, Renormalization group, and Critical phenomena, World Sientific, 1984